

Bremsstrahlung model and the recoil-mass multiplicity distribution in $pp \rightarrow pX$

E. Ugaz

Departamento de Física Teórica, Universidad Autónoma de Barcelona, Bellaterra, Barcelona, Spain

(Received 20 October 1977)

Based on a generalized bremsstrahlung model we obtain a simultaneous average representation of the multiplicity distribution vs missing mass, leading-proton spectrum, and overall prong-distribution data at a fixed incident Fermilab energy. Our results suggest that this simple physical picture, in which a single mechanism underlies both diffractive and nondiffractive regimes, is valid at least in an approximate sense.

I. INTRODUCTION

In this article we present a natural extension of the bremsstrahlung model¹ such that a single physical mechanism underlies the diffractive and nondiffractive regimes in a hadron-induced process. The empirical indication that topological cross sections have a universal character² is the primary motivation in our approach to the extended bremsstrahlung model.³ However, in order to give first a more solid base to the model, a test of its main assumptions should be made as direct as possible. A particularly simple test of this kind, as allowed by the available experimental information, is what we hope to carry out in the present work. We shall thus present a reasonably complete and systematic analysis of the multiplicity distribution of a mass recoiling from a leading hadron.

As far as the universality of prong distributions is concerned, and from a phenomenological point of view, two apparently different types of models (broadly speaking) have been previously presented. The first class are bootstrap models leading to integral-recursion equations for the universal multiplicity distribution.⁴ The second type of model is one based on a multiperipheral picture in which it is assumed that exchanged-particle-proton interactions are similar to on-mass-shell particle-proton collisions.⁵ If, on the one hand, both approaches may not be totally unrelated in the sense that the recursion relation is essentially a multiperipheral equation, on the other hand, an underlying physical mechanism is not clearly identified, especially in the first class of models. Furthermore, the predictive power of these models is somehow diminished as (i) the above-mentioned universality enters as input, (ii) the lead-

ing-particle distribution must be given to determine the bootstrap models, and (iii) no compelling arguments suggest that single-particle exchange dominates for small and large values of the missing mass in models of the multiperipheral type. The bremsstrahlung model is free of these difficulties;³ moreover, we hope to demonstrate that it offers a unified phenomenological scheme for the diffractive and nondiffractive domains at present Fermilab energies (~ 50 – 500 GeV).

In Sec. II we derive the semi-inclusive leading-particle distribution of the bremsstrahlung model. Section III presents an explicit version of the extended bremsstrahlung model with only enough complexity so as to describe the gross features of the data and thus test our basic assumptions as clearly as possible. The systematic comparison of these data with the model predictions is then made in Sec. IV.

II. THE MULTIPLICITY DISTRIBUTION VS MISSING MASS

A derivation of the semi-inclusive leading-particle distribution of the bremsstrahlung model has not been presented before. A brief outline of the main steps leading to this distribution is of interest since this derivation proceeds quite differently from that in Ref. 1. Furthermore, it shall provide a justification for Eq. (2.8b) below which enters crucially in the reasoning³ leading to universal multiplicity distributions in the bremsstrahlung model.

Within the framework of Stodolsky's model, a leading particle behaves analogously to the case of an electron which emits photons in a bremsstrahlung process. If ϵ is the energy lost by one of the incident hadrons, the probability it has radiated N particles, with N_i of them having energy ω_i , is written as

$$P_N(\epsilon) = \sum_{N_1, N_2, \dots} \delta(\epsilon - N_1\omega_1 - N_2\omega_2 - \dots) \delta(N - N_1 - N_2 - \dots) P(N_1)P(N_2) \dots, \quad (2.1a)$$

where

$$P(N_i) = \frac{[(d\bar{N}/d\omega)d\omega]^{N_i}}{N_i!} \exp\left(-\frac{d\bar{N}}{d\omega} d\omega\right) \tag{2.1b}$$

is the probability for N_i emission in the energy interval $\omega_i, \omega_i + d\omega$.

It is convenient to recast (2.1) in the form

$$P_N(\epsilon) = \sum_{N_1 N_2 \dots} \int dt du \exp[-it(\epsilon - N_1\omega_1 - N_2\omega_2 - \dots) - iu(N - N_1 - N_2 - \dots)] \prod_i P(N_i),$$

to obtain

$$P_N(\epsilon) = \int_{-\infty}^{\infty} dt \int_{-\infty}^{\infty} du e^{-i(t\epsilon + uN)} \exp\left[\int_m^{\epsilon} d\omega \frac{d\bar{N}}{d\omega} (e^{i(t\omega + u)} - 1)\right] \exp\left(-\int_{\epsilon}^E d\omega \frac{d\bar{N}}{d\omega}\right),$$

where m is the mass of the primarily radiated unit and the last exponential expresses the fact that no particle is radiated with energy greater than ϵ . Putting $d\bar{N}/d\omega = \lambda/\omega, t = y$, and $\omega/\epsilon = z$, it then follows that

$$P_N(\epsilon) = \frac{1}{\epsilon} \left(\frac{\epsilon}{E}\right)^{\lambda} \left(\frac{m}{\epsilon}\right)^{\lambda} \int_{-\infty}^{\infty} du \exp\left(-iuN + \lambda e^{iu} \ln \frac{\epsilon}{m}\right) \int_{-\infty}^{\infty} dy \exp\left[-iy + \lambda e^{iy} \int_{m/\epsilon}^1 dz (e^{iyz} - 1)/z\right], \tag{2.2}$$

and thus $P_N(\epsilon) \rightarrow 0$ as $\epsilon \rightarrow m$. This threshold behavior must be present in the model in order to smoothly connect with a vanishing probability of radiation if the energy lost gets less than the mass of the primarily radiated unit. Further, for $\epsilon \gg m$, the integration over y is given by

$$\sim \int_{-\infty}^{\infty} dy \exp(-iy + \lambda e^{iy} e^{iy}) = \lambda e^{i\lambda u},$$

and (2.2) takes the form

$$P_N(\epsilon) \approx \frac{\lambda}{\epsilon} \left(\frac{\epsilon}{E}\right)^{\lambda} \frac{[\lambda \ln(\epsilon/m)]^{N-1}}{(N-1)!} \exp[-\lambda \ln(\epsilon/m)], \tag{2.3}$$

where the identity

$$\int_{-\infty}^{\infty} du \exp(iuN + A e^{-iu}) = \frac{A^N}{N!} \tag{2.4}$$

is used.

It is straightforward to show that (2.3) leads to the expression

$$P_N^{(2)}(\epsilon_1, \epsilon_2) = \frac{\lambda^2}{\epsilon_1 \epsilon_2} \left(\frac{\epsilon_1 \epsilon_2}{E_1 E_2}\right)^{\lambda} \frac{[\lambda \ln(\epsilon_1 \epsilon_2 / \bar{m}^2)]^{N-2}}{(N-2)!} \times \exp\left(-\lambda \ln \frac{\epsilon_1 \epsilon_2}{m^2}\right) \tag{2.5}$$

for the probability that the two leading hadrons, with energy losses ϵ_1, ϵ_2 and incident energies E_1, E_2 , respectively, have radiated a total of N particles.

We now write for the semi-inclusive leading-particle distribution,

$$P_N^{(1)}(\epsilon_1, E_2) = \left(\frac{m}{E_2}\right)^{\lambda} P_N(\epsilon_1) + \int_m^{E_2} d\epsilon_2 P_N^{(2)}(\epsilon_1, \epsilon_2),$$

where the probability that the N particles are radiated by the first hadron is given by $(m/E_2)^{\lambda} P_N(\epsilon_1)$. Thus

$$P_N^{(1)}(\epsilon_1, E_2) = \frac{\lambda}{\epsilon_1} \left(\frac{\epsilon_1}{E_1}\right)^{\lambda} \frac{[\lambda \ln(\epsilon_1 E_2 / m^2)]^{N-1}}{(N-1)!} \times \exp\left(-\lambda \ln \frac{\epsilon_1 E_2}{m^2}\right). \tag{2.6}$$

The sum over N in (2.6) gives then¹

$$P^{(1)}(\epsilon_1, E_2) = \frac{\lambda}{\epsilon_1} \left(\frac{\epsilon_1}{E_1}\right)^{\lambda}. \tag{2.7}$$

Since experimental quantities are given in terms of the missing mass M^2 and the Feynman scaling variable x , we write the leading inclusive cross section (2.7) as

$$\frac{d\sigma}{dx} = \sigma \lambda (1 - |x|)^{\lambda-1}, \tag{2.8a}$$

and the semi-inclusive leading-particle distribution (2.6) as

$$\frac{d\sigma_N}{dx} = \frac{d\sigma}{dx} \frac{[\lambda \ln(M^2/s_0)]^{N-1}}{(N-1)!} \exp\left(-\lambda \ln \frac{M^2}{s_0}\right), \tag{2.8b}$$

both expressions valid for

$$|x| \leq 1 - s_0/s \tag{2.8c}$$

and where we used, in the c.m. system,

$$\frac{\epsilon_1}{E_1} \approx 1 - |x|, \quad \frac{\epsilon_1 E_2}{m^2} \approx \frac{s(1 - |x|)}{4m^2} \approx \frac{M^2}{s_0}, \tag{2.9a}$$

$$s_0 \equiv 4m^2. \tag{2.9b}$$

From (2.8b) the N -particle production cross section will be

$$\begin{aligned} \sigma_N(s) &= \int_0^{1-s_0/s} dx \frac{d\sigma_N}{dx} \\ &= \sigma \frac{[\lambda \ln(s/s_0)]^N}{N!} \exp\left(-\lambda \ln \frac{s}{s_0}\right), \end{aligned} \tag{2.10a}$$

and the average multiplicity

$$\bar{N}(s) = \lambda \ln \frac{s}{s_0}. \quad (2.10b)$$

Equations (2.8) and (2.10a) lead trivially to universality of multiplicity distributions.³

III. THE MODEL

We shall consider in this section a generalized bremsstrahlung model in which the incoming hadrons incoherently radiate two different cluster species. If the effective mass of one of the species is very light, thereby allowing low-mass radiation in the small- M^2 region, the model is naturally extended into the diffractive regime.

Let these two components be characterized by λ_1, λ_2 and have effective threshold masses $s_0(\lambda_1) \equiv s_1 \ll s_0(\lambda_2) \equiv s_2$. Then we write directly from (2.8) and (2.10),

$$\frac{d\sigma}{dx} = \begin{cases} \frac{d\sigma_1}{dx}, & |x| \geq 1 - s_2/s, \\ \sum_{i=1}^2 \frac{d\sigma_i}{dx}, & |x| \leq 1 - s_2/s, \end{cases} \quad (3.1a)$$

$$\frac{d\sigma_N}{dx} = \begin{cases} \frac{1}{\bar{\sigma}_1} \frac{d\sigma_1}{dx} \sigma_{N-1}^{(1)}(s(1-x)), & |x| \geq 1 - s_2/s, \\ \sum_{i=1}^2 \frac{1}{\bar{\sigma}_i} \frac{d\sigma_i}{dx} \sigma_{N-1}^{(i)}(s(1-x)), & |x| \leq 1 - s_2/s, \end{cases} \quad (3.1b)$$

$$\sigma_N(s) = \sum_{i=1}^2 \sigma_N^{(i)}(s), \quad s \geq s_2, \quad (3.1c)$$

$$\bar{N}(s) = \sum_{i=1}^2 \frac{\bar{\sigma}_i}{\sigma} \lambda_i \ln \frac{s}{s_i}, \quad s \geq s_2, \quad (3.1d)$$

where

$$d\sigma_i/dx = \bar{\sigma}_i \lambda_i (1 - |x|)^{\lambda_i - 1}, \quad (3.1e)$$

$$\sigma_N^{(i)}(z) = \bar{\sigma}_i \frac{[\lambda_i \ln(z/s_i)]^N}{N!} \exp\left(-\lambda_i \ln \frac{z}{s_i}\right), \quad (3.1f)$$

and $\bar{\sigma}_1, \bar{\sigma}_2$ are inelastic cross sections belonging to each component. The normalization is to the total inelastic cross section

$$\sigma_0 + \int_0^{1-s_1/s} dx d\sigma/dx = \bar{\sigma}_1 + \bar{\sigma}_2 = \sigma. \quad (3.1g)$$

We realize that this will be an over-idealized picture. In particular, the absence of threshold

factors which make a given component vanish as $M^2 \rightarrow s_i$ (see Sec. II) and the presence of only one component in the small- M^2 region, do not permit a smooth transition between the diffractive and nondiffractive regimes. Clearly, we have considered only two components in the spirit of simplicity. In spite of the simplifications used, however, this model does have other interesting characteristic features³ besides simplicity. Notice, especially, that universality is preserved since each cluster component obeys a bootstrap relation of the form

$$\sigma_N^{(i)}(s) = \int_0^{1-s_i/s} dx \frac{1}{\bar{\sigma}_i} \frac{d\sigma_i}{dx} \sigma_{N-1}^{(i)}(s(1-x)). \quad (3.2)$$

Furthermore, the model provides, as we shall see, a simple interpretation of data at present Fermilab energies.

A. Final-state particles

The second component does not enter in the diffractive region, so it is sensible to identify it with the central clusters of multihadron production. From the clustering properties of the final-state hadrons in two-particle inclusive reactions, the average properties of the heavy cluster are fairly well determined.⁶ For definiteness, then, we assume that (i) $m_2 \sim 2$ GeV and from (2.9b) $s_2 \approx 18$ GeV², (ii) this cluster always decays into exactly two charged particles, $\bar{N}_2 = 2$ (\bar{N}_2 is the mean number of charged hadrons in the heavy cluster), and (iii) $\lambda_2 \sim 1$.

As the second component must be dominant in the central region $\lambda_1 \ll \lambda_2$, so these parameters have been essentially fixed. Also, the diffractive and nondiffractive cross sections at 205 GeV/c are taken as $\bar{\sigma}_1 \approx 6.6$ mb (Ref. 7) and $\bar{\sigma}_2 \approx 25.4$ mb, respectively, with $\sigma = \bar{\sigma}_1 + \bar{\sigma}_2 \approx 32$ mb as the total inelastic cross section.⁸

We leave as free parameters the mass $s_1 = 4m_1^2 \ll s_2$, and the decay multiplicity distribution of the light cluster. For the sake of simplicity we assume this cluster can only decay either into two charged hadrons with probability p or into neutrals with probability $1-p$. This leads to $\bar{N}_1 = 2p$ as the average number of charged particles in the light cluster.

Standard manipulations on (3.1b) and (3.1c), with the assumptions given before, determine then

$$\frac{d\sigma_{n_c=2n+1}}{dx} = \begin{cases} \frac{d\sigma_1}{dx} \left[\frac{N_1}{2} \frac{[(\bar{N}_1/2)\lambda_1 \ln(M^2/s_1)]^{n-1}}{(n-1)!} + \left(1 - \frac{\bar{N}_1}{2}\right) \frac{[(\bar{N}_1/2)\lambda_1 \ln(M^2/s_1)]^n}{n!} \right] \exp\left(-\frac{\bar{N}_1}{2} \lambda_1 \ln \frac{M^2}{s_1}\right), & |x| \geq 1 - s_2/s, \\ \sum_{i=1}^2 \frac{d\sigma_i}{dx} \left[\frac{\bar{N}_i}{2} \frac{[(\bar{N}_i/2)\lambda_i \ln(M^2/s_i)]^{n-1}}{(n-1)!} + \left(1 - \frac{\bar{N}_i}{2}\right) \frac{[(\bar{N}_i/2)\lambda_i \ln(M^2/s_i)]^n}{n!} \right] \exp\left(-\frac{\bar{N}_i}{2} \lambda_i \ln \frac{M^2}{s_i}\right), & |x| \leq 1 - s_2/s, \end{cases} \quad (3.3a)$$

$$\sigma_{n_c=2n+2}(s) = \sum_{i=1}^2 \bar{\sigma}_i \frac{[(\bar{N}_i/2)\lambda_i \ln(s/s_i)]^n}{n!} \exp\left(-\frac{\bar{N}_i}{2}\lambda_i \ln \frac{s}{s_i}\right), \quad s \geq s_2, \quad (3.3b)$$

$$\bar{n}_c(s) = 2 + \sum_{i=1}^2 \frac{\lambda_i \bar{\sigma}_i}{\sigma} \bar{N}_i \ln \frac{s}{s_i}, \quad s \geq s_2, \quad (3.3c)$$

where n_c is the number of final-state charged hadrons. The experimental results for $d\sigma_{n_c}/dx$ to be considered in Sec. IV are given in an integrated (over M^2 intervals) form, in which case

$$P_{n_c} = (M_2^2 - M_1^2)^{-1} \int_{M_1^2}^{M_2^2} dM^2 \sigma^{-1} d\sigma_{n_c}/dx \quad (3.3d)$$

is to be compared with experiment.

Given Eqs. (3.3) one can write the x -dependent average charged multiplicity,

$$\bar{n}_c(x) = \sum_{n=0}^{\infty} (2n+1) d\sigma_{n_c}/dx (d\sigma/dx)^{-1},$$

as

$$\bar{n}_c(x) = \begin{cases} 1 + \bar{N}_1 + \bar{N}_1 \lambda_1 \ln \frac{M^2}{s_1}, & |x| \geq 1 - s_2/s, \\ 1 + \sum_{i=1}^2 \frac{d\sigma_i/dx}{d\sigma/dx} \left(\bar{N}_i + \bar{N}_i \lambda_i \ln \frac{M^2}{s_i} \right), & |x| \leq 1 - s_2/s, \end{cases} \quad (3.4)$$

where the terms not containing $\ln(M^2/s_i)$, apart from the unity representing a proton, arise because, for any $|x| \leq 1 - s_i/s$, a single cluster, at least, must have been radiated.

IV. PHENOMENOLOGICAL APPLICATION

In order to compare experiment and theory, we shall use the $pp \rightarrow X$ and $pp \rightarrow p+X$ data at 205 GeV/c which have been extensively studied⁹⁻¹¹ in a form suitable for our purposes.

A. The diffractive region

According to the model of Sec. III the diffractive regime roughly corresponds to $M^2 \leq s_2$ or $|x| \geq 0.95$. As previously said a one-component dominance in this region is an approximation. Effective mass distributions show evidence of a substantial amount of resonance production in diffraction dissociation at Fermilab energies.² Also, a diffractive contribution is visible as a low-mass peak in events with six or fewer charged prongs.⁹ A detailed description of these data, within the view presented in Sec. III, presumably requires a careful treatment of the low- and medium-mass radiation regions, resembling more a continuous emission of low-mass clusters than the emission of a single component used in the present work.

We shall limit ourselves, therefore, with an average description of the P_{n_c} and $d\sigma/dx$ 205 GeV/c diffractive data in the region $M^2 \leq 10$ GeV². This is shown in Figs. 1(a) and 2 ($|x| \rightarrow 1$ region) where we have used $\lambda_1 \approx 0.07$, $s_1 \approx 1$ GeV², and $\bar{N}_1 \approx 0.90$. Because of the requirements $\lambda_1 \ll 1$ and $s_1 \ll s_2$, this set of parameters is fairly well fixed within small limits.

Although the predicted distribution P_{n_c} seems adequate for $0 < M^2 < 10$ GeV², a closer look would reveal no more than rough agreement with data¹⁰ in each of the separate regions $0 < M^2 < 5$ GeV² and $5 < M^2 < 10$ GeV². This situation is also reflected in $d\sigma/dx$ for $|x|$ near one. The distribution (3.1a) decreases too rapidly resulting in a very sharp diffractive peak as displayed in Fig. 2. Had we considered another component λ'_1 for the diffractive region, representing medi-

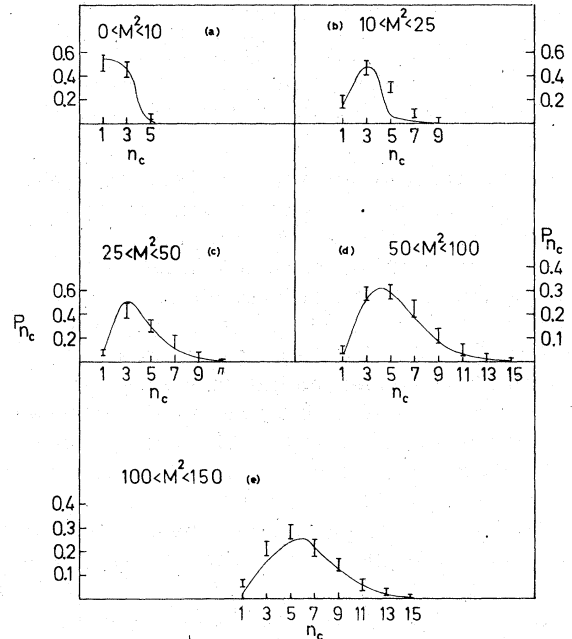


FIG. 1. Multiplicity distribution of the system X in $pp \rightarrow pX$ at 205 GeV/c. Data points (Ref. 10) are the probabilities P_{n_c} to produce n_c charged particles. Data for $0 < M^2 < 5$ GeV² and $5 < M^2 < 10$ GeV² have been combined together into a single region $0 < M^2 < 10$ GeV². Solid lines are computed from (3.3d). (a) For $0 \leq M^2 \leq 10$ GeV² the diffractive component alone contributes. (b) In this M^2 interval, the nondiffractive component is also present for $18 \leq M^2 \leq 25$ GeV². (c)–(e) For this range of M^2 values both components contribute.

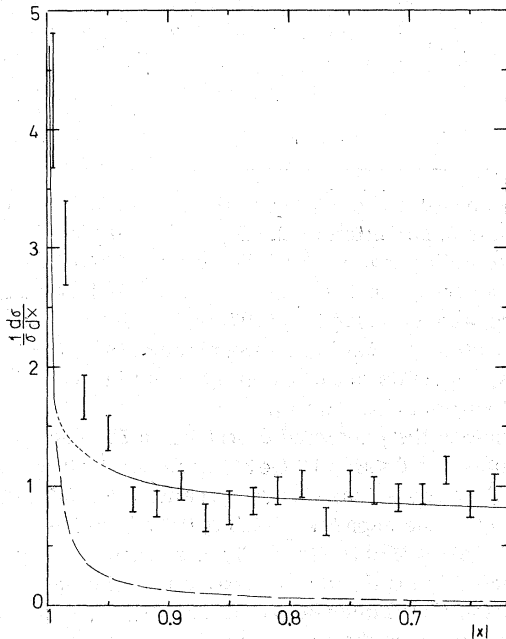


FIG. 2. Leading-particle spectrum at 205 GeV/c. Experimental points are from Ref. 9. The long-dashed curve is the diffractive component alone. The solid curve is the prediction of the model in Sec. III [Eq. (3.1a)] which has two contributions, except for $|x| \sim 1$ where only the diffractive component is present. The nondiffractive component contributes up to $|x| \sim 0.95$. As discussed in the text, the model is not expected to hold in the transition region (short-dashed curve).

um-mass radiation and with $\lambda_1 < \lambda'_1 < \lambda_2$, this peak would become much broader providing a smoother connection between the diffractive and nondiffractive regimes. As present data for the transition region are too scant to examine in detail [see Fig. 1(b) and the short-dashed line region in Fig. 2] we defer in the present work a more quantitative statement on this possibility. It seems, nevertheless, that a more detailed model for the transition region would be more sensitive to the $d\sigma/dx$ data than to P_{nc} , as Figs. 1(b) and 2 suggest.

It is interesting, anyhow, that the gross features of the diffractive peak and multiplicity distribution at small M^2 can both be represented by a physical picture of low-mass hadronic bremsstrahlung. Certain consequences follow from our analysis which, in spite of the simplifications used, seem to have greater validity than the specific context employed to arrive at them. The coupling constant λ_1 characteristic of low-mass emission is very small, perhaps diminishing as the mass of the radiated object decreases. Thus the M^{-2} diffractive falloff can be extended down to small values of M^2 in which a triple-Pomeron analysis

would not be expected to hold. In particular, for $4 < M^2 < 9 \text{ GeV}^2$ and with $\lambda_1 \approx 0.07$ the predicted invariant cross section $M^2 d\sigma/dM^2$ is essentially independent of M^2 and compatible with recent high-statistics data at Fermilab energies.¹² There is also a suggestion that "leading" and "central" clusters have different mass ($s_1 \ll s_2$) and internal charged distribution ($\bar{N}_1 \sim \frac{1}{2} \bar{N}_2$). This suggestion is reinforced below when the $\bar{n}_c(x)$ data is examined for $|x|$ near 1. It should be valuable to see if there is any connection at all between the leading clusters of this work and the large leading cluster effect observed in π^-p vs pp reactions.^{2, 13}

B. Other predictions

The flattening of the curve in Fig. 2 at $|x| \sim 0.9$ is striking, and was the initial impetus for the bremsstrahlung model.¹ For definiteness we let $\lambda_2 = 1 - \lambda_1$ to obtain the solid curve of Fig. 2 in the region $0.6 \leq |x| \leq 0.95$. We can see from this figure that the second component is flat and dominant throughout this $|x|$ interval. In addition to this fit one also has, (i) a simultaneous description of the semi-inclusive leading spectrum as a function of n_c and M^2 , Figs. 1(c)–1(e), (ii) a universal multiplicity distribution, i.e., the even-prong probabilities obtained from $pp \rightarrow X$ at fixed $s \approx M^2$ smoothly alternate¹⁰ with the odd prongs in Fig. 1 (see also Fig. 3 for the overall multiplicity distribution at 205 GeV/c and further discussion below), and (iii) an underlying physical picture, of attractive simplicity, common to both diffractive and nondiffractive domains.

The qualitative features of the data in Figs. 1, 2, and 3 are thus compatible with the model. Some discrepancies, however (mainly at a level of $\sim 20\%$ accuracy), are worth mentioning. Our approximation that the heavy cluster always decays into exactly two charged particles may be questionable to some degree, as the data in Figs.

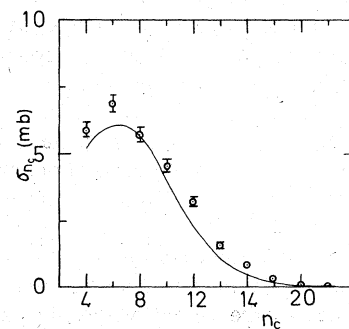


FIG. 3. The multiplicity distribution at 205 GeV/c. Data are from Ref. 11 and only for $n_c \geq 4$ where the nondiffractive contribution is dominant. The solid curve is predicted from (3.3b).

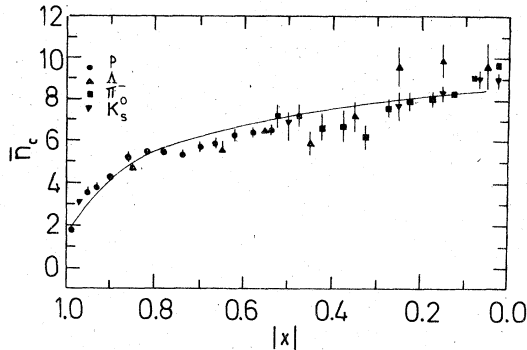


FIG. 4. The average charged multiplicity, in $pp \rightarrow pX$ at 205 GeV/c, as a function of $|x|$. The solid curve is the theoretical prediction of the model as given in (3.4). Data points are from Ref. 9. Besides the solid circles, we include data where the observed particle is other than the leading proton.

1(c)–1(e) and 3 seem to indicate. In fact a better fit to the larger M^2 , smaller n_c, P_{n_c} data can be obtained if one allows for a small probability that this cluster decays into neutrals, e.g., with $\bar{N}_2 \approx 1.70$ instead of the value 2.0 used here.³ Nevertheless, in order to provide a cleaner test for the main assumptions in the model, we have kept the simpler choice $\bar{N}_2 = 2$. One also expects that the diffractive component, and the approximations made upon it, is more sensitive at smaller n_c . The predicted average charged multiplicity at 205 GeV/c is $\bar{n}_c \approx 6.7$ ($\bar{n}_c^{\text{exp}} \approx 7.5$). Overall, there is a suggestion from these fits that the non-diffractive regime is better approximated by a single component than the diffractive one.

The comparison of the model with the average charged multiplicity data⁹ as a function of x is displayed in Fig. 4. The solid curve, predicted from (3.4), has some noteworthy features. As $|x| \rightarrow 1$, $\bar{n}_c(x) \rightarrow 1 + \bar{N}_1$, i.e., the proton and the \bar{N}_1 charged hadrons resulting from the decay of a singly radiated light cluster. The data suggest $\bar{N}_1 \approx 0.9$ in agreement with the value found before from the P_{n_c} data. The downward curvature of the multiplicity as $|x|$ increases is also nicely reproduced by the model.

Notice that some of the data points in Fig. 4 correspond to the average charged multiplicity as a function of x for inclusive Λ , π^- , and K_S^0 production in pp interactions at 205 GeV/c.⁹ The predicted $\bar{n}_c(x)$, down to $x \sim 0$, agrees roughly with these data. Thus the model seems compatible with the experimental suggestion that the average charged multiplicity associated with the mass recoiling from a given particle appears to depend only on the x value of the observed particle. The model prediction, as described in the Appen-

dix, for the average charged multiplicity $\bar{n}_{c,A}(x)$ of the process $pp \rightarrow A + X$, where A is a final-state hadron other than the leading proton, leads to a natural interpretation of this regularity. The essence of this result might be seen on the basis that the Poissonian relation, $(\lambda d\omega/\omega)^{N+1}/(N+1)!$, to radiate $N+1$ clusters of energy ω [see (2.1b)], remains Poissonian after any one of them is singled out, $\lambda d\omega/\omega (\lambda d\omega/\omega)^N/N!$. This implies that the leading proton-cluster spectrum has essentially the structure of (2.8b) where, as expected, M^2 is the missing mass of the system under consideration. The average multiplicity as a function of x is thus of the same basic form as before. (See Appendix for a more detailed discussion.)

Because the second component is dominant as soon as the energy of the system is larger than s_2 , from (3.3c) and (3.4) we have

$$\bar{n}_c(s) \underset{s \gg s_2}{\sim} \bar{N}_2 \lambda_2 \ln \frac{s}{s_2}$$

and

$$\bar{n}_c(M^2) \underset{M^2 \gg s_2}{\sim} \bar{N}_2 \lambda_2 \ln \frac{M^2}{s_2},$$

implying universal average multiplicities for the final-state hadrons. On the other hand, it is necessary that $M^2, s \gg s_2$ so that (3.3a) and (3.3b) also obey a bootstrap relation of the form (3.2). Within the assumptions of the present work, final-state universality is thus a general prediction of the bremsstrahlung model in the energy scale $M^2, s \gg s_2$. However, because $\bar{N}_2 = 2$, the second component in (3.3a) and (3.3b) obeys exactly the bootstrap relation at all energies indicating that final-state universality is already expected in the energy range $M^2 \gtrsim s_2$. This is in accord with the previously mentioned experimental evidence for a smooth interpolation of the even-prong probabilities from $pp \rightarrow X$ with the odd prongs in Fig. 1.

V. CONCLUSIONS

In the present work we have been mostly concerned with the multiplicity distribution of a mass recoiling from a leading hadron in high-energy proton interactions. The leading-proton spectrum and overall prong distribution at a given incident energy were also simultaneously considered. In order to provide a simple and unified interpretation of data in both diffractive and nondiffractive domains a natural extension of the bremsstrahlung model was found adequate. The clue to consider the bremsstrahlung model as a potential candidate with this unifying characteristic lies in its ability to predict a universal multiplicity distribution

for the primarily radiated units.

Thus, in the model, a single physical mechanism (hadronic bremsstrahlung) underlies multihadron production in the diffractive and nondiffractive regimes. At low values of the missing mass, when only the radiation of a light cluster (π, ρ, \dots ?) is allowed, one has a physical picture of diffraction not substantially different from the picture present at larger values of M^2 , where a heavier cluster can simultaneously be radiated. We stress that this framework seems potentially rich for a larger range of values in missing mass than those considered in the present work as it is reminiscent of the usual two-component model of multihadron production. The gross features of the data at present Fermilab energies are consistent, in particular, with the universal character of multiplicities predicted by the model.

The assumption of a single dominant component in each of the diffractive and nondiffractive domains was clearly a simplification. This approximation seemed more adequate for the nondiffractive component. Other characteristics of the model, such as the decay properties of clusters, were kept as simple as possible. It is not surprising then that the model fails to account for more detailed features of the data. Besides, no attempt was made to incorporate into the model either threshold factors or how the components might behave over a wider range of energy than the present Fermilab regime.

Our results suggest that the leading and central clusters of the model have distinct structures. From an experimental point of view, there is a hint for such an expectation in the average multiplicity data $\bar{n}_c(x)$ near $x=1$. Here, a single light cluster is essentially being radiated and $\bar{n}_c(x)$ depends on the average number of charged pions in the light cluster. Experiment shows that this number is close to 1, rather than the number 2 expected for central clusters. Accurate measurements of topological cross sections and correlations in the diffractive region can provide, in principle, a more reliable test.

The experimental indication that hadronic multiplicities in $pp \rightarrow$ final-state hadron + X are all universal seems also to have a natural interpretation in the bremsstrahlung model. Detailed data of this sort are of obvious interest to test universality and to elucidate the decay structure of cluster \rightarrow final-state hadron + anything. This structure should be consistent with what one has learned from correlations in the central region.

APPENDIX

We shall briefly illustrate here the calculation of the average charged multiplicity of the system

X in $pp \rightarrow A + X$ where particle A is a hadron other than the leading proton. The radiation of only a single cluster species shall be considered.

By a parallel derivation as that leading to Eq. (2.8) one arrives at a leading proton-cluster semi-inclusive spectra.

$$\frac{z}{\sigma} \frac{d\sigma_N}{dw dz} \approx \lambda^2 (1-w-z)^{\lambda-1} \frac{\{\lambda \ln[s(1-w-z)/s_0]\}^{\lambda-1}}{(N-1)!} \times \exp\left[-\lambda \ln \frac{s(1-w-z)}{s_0}\right], \quad (A1)$$

where w and z are the scaling variables of the leading proton and cluster, respectively, both of them in the same (forward) hemisphere. The inclusive spectrum is then¹⁴

$$\frac{z}{\sigma} \frac{d\sigma}{dw dz} \approx \lambda^2 (1-w-z)^{\lambda-1}. \quad (A2)$$

As in the case of (2.8b), $d\sigma_N/dw dz$ must be a function of $(N-1)$ for arbitrary w and z . From (A1) the semi-inclusive cluster distribution will be

$$z \frac{d\sigma_N}{dz} = \int_0^{1-s_0/s-z} dw z \frac{d\sigma_N}{dw dz},$$

that is,

$$\frac{z}{\sigma} \frac{d\sigma_N}{dz} = \lambda (1-z)^\lambda \frac{\{\lambda \ln[s(1-z)/s_0]\}^{\lambda-1}}{(N-1)!} \times \exp\left[-\lambda \ln \frac{s(1-z)}{s_0}\right]. \quad (A3)$$

In Eqs. (2.8b), (A1), and (A3) the missing mass is always the relevant variable, independently of which reaction $pp \rightarrow p + X_N$, $pp \rightarrow p + \text{cluster} + X_N$ or $pp \rightarrow \text{cluster} + X_N$ is being considered.

In order to obtain a final-state-particle distribution, the convolution of the cluster decay spectrum for particle A , $u dN_A/du$ ($u = p_A^||/p_{\text{cluster}}^||$), with (A3) is taken in the usual way

$$x \frac{d\sigma_N^{(A)}}{dx} = \int \frac{du}{u} z \frac{d\sigma_N}{dz} \Big|_{z=x/u} u \frac{dN_A}{du}. \quad (A4)$$

The average charged multiplicity $\bar{n}_{c,A}(x)$ for $pp \rightarrow A + X$ is thus obtained as in (3.4c),

$$\bar{n}_{c,A}(x) = 2 + \lambda \bar{N} \left[\int_x^1 du \frac{dN_A}{du} \lambda \left(1 - \frac{x}{u}\right)^\lambda \times \ln \frac{s[1 - (x/u)]}{s_0} \right] \times \left[\int_x^1 du \frac{dN_A}{du} \lambda \left(1 - \frac{x}{u}\right)^\lambda \right]^{-1}, \quad (A5)$$

where \bar{N} is the mean number of charged particles in the decay of a single cluster.

We are interested in a rough understanding of

the $\bar{n}_{c,A}(x)$ data of Fig. 4 so that an approximate estimation of (A5) is adequate. Since a single cluster component is dominant either in the diffractive region or for $|x| \lesssim 0.9$, let us illustrate the reasoning involved in the case of the central region where the decay properties of the heavy clusters are better known. For the central cluster the inclusive one-pion decay distribution (in rapidity) is a Gaussian centered at the cluster rapidity with a width less than one unit.⁶ In the case of heavy particles this distribution may be much narrower than that for pions.¹⁵ Therefore, for both x and u in the *central region*, one finds that dN_A/du is peaked at $u \sim 1$, and it is safe to simply write (A5) as

$$\bar{n}_{c,A}(x) \sim 2 + \lambda_2 \bar{N}_2 \ln \frac{s(1-x)}{s_2}. \quad (\text{A6})$$

[With a linear spectrum $dN_A/du \sim u$, for example, (A6) differs from (A5) by less than $\sim 10\%$.]

On the other hand, in the region $|x| \lesssim 0.9$, we have from (3.4)

$$\bar{n}_c(x) \sim 1 + \bar{N}_2 + \lambda_2 \bar{N}_2 \ln \frac{s(1-x)}{s_2}, \quad (\text{A7})$$

where only the dominant second component has been considered. One can see that (A6) and (A7) have the same form and are of comparable magnitude, the difference is less important as $M^2 = s(1-x)$ becomes much larger than s_2 .

¹L. Stodolsky, Phys. Rev. Lett. **28**, 60 (1972).

²For a recent review see, for example, J. Whitmore, Phys. Rep. **27C**, 187 (1976).

³E. Ugaz, following paper, Phys. Rev. D **17**, 2483 (1978).

⁴A. Krzywicki, invited lecture at the International Summer Institute in Theoretical Physics, Bielefeld, 1976 [Orsay report (unpublished)]; R. Jengo, A. Krzywicki and B. Peterson, Nucl. Phys. **B65**, 319 (1973); A. Morel and B. Peterson, *ibid.* **B91**, 109 (1975).

⁵G. C. Fox, in *High Energy Collisions—1973*, proceedings of the Fifth International Conference, Stony Brook, edited by C. Quigg (AIP, New York, 1973).

⁶For a review and references, see G. H. Thomas, invited talk at the International Summer Institute in Theoretical Physics, Bielefeld (Argonne report, 1977) (unpublished).

⁷J. W. Chapman *et al.*, Phys. Rev. Lett. **32**, 257 (1974).

⁸G. Giacomelli, Phys. Rep. **23C**, 123 (1976).

⁹J. Whitmore *et al.*, Phys. Rev. D **11**, 3124 (1975).

¹⁰J. Whitmore and M. Derrick, Phys. Lett. **50B**, 280 (1974).

¹¹S. Barish *et al.*, Phys. Rev. D **9**, 2689 (1974).

¹²D. S. Ayres *et al.*, Phys. Rev. Lett. **37**, 1724 (1976).

¹³W. D. Shephard, talk presented at the VII International Colloquium on Multiparticle Dynamics, Tutzing, 1976 (unpublished).

¹⁴J. Benecke, talk presented at XVIII International Conference on High Energy Physics, Tbilisi, 1976 (unpublished).

¹⁵A. Bialas, M. Jacob, and S. Pokorski, Nucl. Phys. **B75**, 259 (1974).